



Retroductal Nanoparticle Injection to the Murine Submandibular Gland

Jomy J. Varghese¹, Isaac L. Schmale², Yuchen Wang¹, M. Eva Hansen¹, Shawn D. Newlands², Catherine E. Ovitt³, and Danielle S.W. Benoit¹

Jomy J. Varghese: Jomy_varghese@urmc.rochester.edu; Isaac L. Schmale: Isaac_Schmale@urmc.rochester.edu; Yuchen Wang: Yuchen_Wang@urmc.rochester.edu; M. Eva Hansen: Mhansen9@u.rochester.edu; Shawn D. Newlands: Shawn_Newlands@urmc.rochester.edu; Catherine E. Ovitt: Catherine_ovitt@urmc.rochester.edu; Danielle S.W. Benoit: danielleswbenoit@rochester.edu

¹Department of Biomedical Engineering, University of Rochester, Rochester, NY, USA

²Department of Otolaryngology Head and Neck Surgery, University of Rochester Medical Center, Rochester, NY, USA

³Center for Oral Biology, University of Rochester Medical Center, Rochester, NY, USA

Abstract

SHORT ABSTRACT—Local drug delivery to the submandibular glands is of interest in understanding salivary gland biology and for the development of novel therapeutics. We present an updated and detailed retroductal injection protocol, designed to improve delivery accuracy and experimental reproducibility. The application presented herein is the delivery of polymeric nanoparticles.

LONG ABSTRACT—Two common goals of salivary gland therapeutics are prevention and cure of tissue dysfunction following either autoimmune or radiation injury. By locally delivering bioactive compounds to the salivary glands, greater tissue concentrations can be safely achieved versus systemic administration. Furthermore, off target tissue effects from extra-glandular accumulation of material can be dramatically reduced. In this regard, retroductal injection is a widely used method for investigating both salivary gland biology and pathophysiology. Retroductal administration of growth factors, primary cells, adenoviral vectors, and small molecule drugs has been shown to support gland function in the setting of injury. We have previously shown the efficacy of a retroductally injected nanoparticle-siRNA strategy to maintain gland function following irradiation. Here, a highly effective and reproducible method to administer nanomaterials to the murine submandibular gland through Wharton's duct is detailed (Figure 1). We describe accessing the oral cavity and outline the steps necessary to cannulate Wharton's duct, with further observations serving as quality checks throughout the procedure.

Keywords

Cannulation; retrograde; retroductal; nanoparticle; submandibular; salivary; gland

CORRESPONDING AUTHORS: Danielle S.W. Benoit, Catherine E. Ovitt.

A complete version of this article that includes the video component is available at <http://dx.doi.org/10.3791/57521>.

DISCLOSURES: The authors have nothing to disclose.

INTRODUCTION

Salivary gland dysfunction has many etiologies, including Sjögren's syndrome, an autoimmune mediated loss of functional secretory tissue, and radiation induced hyposalivation (RIH), a common sequella of head and neck cancer radiotherapy¹. Loss of salivary function due to either condition predisposes individuals to oral and systemic infection, tooth decay, digestive and swallowing dysfunction, speech impairment, and major depression¹⁻³. As a result, quality of life significantly suffers, with interventions limited to palliation of symptoms rather than cure⁴. To investigate novel therapies *in vivo*, it is of interest to administer bioactive compounds directly to the salivary gland.

Retroductal injection is a valuable method to deliver bioactive compounds directly to the salivary glands and test the efficacy in disease, injury, or under normal tissue homeostasis. The three major salivary glands are the parotid (PG), the submandibular (SMG), and the sublingual (SLG), all of which empty into the oral cavity through excretory ducts. The anatomy of the murine SMG permits direct access through cannulation of Wharton's duct, located in the floor of the mouth beneath the tongue⁵. Following the cannulation, solvated drugs can be administered directly to the SMG. Following retroductal delivery, extra-glandular diffusion is restricted by the surrounding tissue capsule which regulates the exchange of material with surrounding structures⁶. The SMG and its duct are similarly structured in humans, and are routinely accessed during SMG surgery and sialoendoscopy⁷. In humans and mice, the PG is likewise accessible via Stensen's duct in the buccal mucosa⁸.

In murine models of RIH, SMG retroductal injection has been used to deliver therapeutics including growth factors, primary cells, adenoviral vectors, cytokines, and antioxidant compounds to modulate the cellular response to injury, and reduce the resulting tissue damage^{5,9-16}. The most notable clinical success of retroductal injection is the administration of adenoviral vector to direct expression of a water channel (Aquaporin 1; AQP1) in patients following the radiation for head and neck cancer¹⁷.

Previously, we have developed and shown the efficacy of a retroductally injected polymeric nanoparticle-siRNA system to protect salivary gland function from RIH^{11,18-20}. As an extension of our past work, here, we demonstrate our protocol for retroductal SMG injection using a fluorescently labeled nanoparticle (NP) capable of loading and delivering otherwise poorly soluble drugs²¹⁻²³.

We have synthesized the NP from a diblock copolymer comprised of poly(styrene-alt-maleic anhydride)-b-poly(styrene) (PSMA) through reversible addition chain fragmentation (RAFT) polymerization, as described previously²¹. Through solvent exchange, these polymers spontaneously self-assemble into micelle NP structures with a hydrophobic interior and hydrophilic exterior²¹. The NPs are labeled with Texas-Red fluorophore to permit the verification of NP delivery into the glands without sacrificing the animal. Live animal imaging and SMG immunohistochemistry is shown at 1 h and 1 day following the injection.

This updated and reproducible cannulation protocol should enable others to achieve retroductal injection. We expect that this refined technique will become critical for *in vivo* studies and therapeutic development^{24,25}.

PROTOCOL

All *in vivo* procedures outlined below were approved by the University Committee on Animal Resources at the University of Rochester, Rochester, NY.

1. Preparation

- 1.1 . Using 32G intracranial catheter tubing with wire inset, cut 3 cm of the tubing to form a beveled end, approximately 45° to the long axis. Confirm that the wire is at least 1 cm longer than the tubing.
- 1.2 Load 50 µL of PSMA nanoparticle solution (Figure 1), or other injection material, into a Hamilton syringe. To reduce the probability of barotrauma during injection, attach the catheter tubing, with the stylet removed, to the syringe and expel dead volume.
- 1.3 Inspect the injection solution to ensure the nanoparticle is fully solvated to prevent ductal obstruction following the administration.
- 1.4 Prepare atropine solution at 0.1 mg/mL.

Note: Because atropine is light sensitive and degrades over time, this solution should be made the day of injection, and protected from light until administered.

2. Accessing and Visualizing Ductal Entry Point

- 2.1 Weigh C57/B16 mice using an analytical balance.
- 2.2 Using a 0.5 mL syringe with 29G × ½" needle, anesthetize mice with an intraperitoneally injected sterile saline solution of 100 mg/kg ketamine and 10 mg/kg xylazine. Proceed to the following step when the mouse no longer responds to stimuli, which generally occurs within 5 to 10 min following the injection.

Note: This procedure may also be performed under isoflurane, but will require a custom nose cone that permits access to the oral cavity.

- 2.3 To prevent dryness during the procedure, apply lubricant to eyes and place the mouse in a prone position on a custom stage.

Note: To maintain appropriate conditions for intra-oral procedure, tools should be disinfected or sterilized prior to each use.

- 2.4 Open the oral cavity by securing the maxillary incisors over a metal beam, and use an elastic band to apply downward tension behind the mandibular incisors (Figure 2A).
- 2.5 Align the mouse beneath the dissecting microscope such that the base of the jaw is visualized.

- 2.6 To widen the mouth, use a custom, curved steel retractor to apply tension bilaterally to the buccal mucosa.
- 2.7 To visualize the submandibular papillae, grasp and gently lift the tongue from the floor of the mouth using blunt forceps.

Note: The papillae will appear as two pale protrusions beneath the tongue (Figure 2B).

- 2.8 To ease the visualization and further manipulation within the oral cavity, place cotton between the tongue and the buccal mucosa.

3. Ductal Cannulation and Line Placement

- 3.1 Using fine, curved forceps, grasp catheter tubing with the wire inset. For optimum manual control during cannulation, align the tubing with the curvature of the forceps (Figure 3A).
- 3.2 Using the dissecting microscope, move the forceps and wire into the field of view.

Note: The wire should be protruding from the tubing.
- 3.3 Gently apply pressure into the base of one submandibular papilla using the wire inset to produce a small, superficial, mucosal puncture (0.076 mm diameter) that will facilitate later entry of the catheter tubing (0.25 mm diameter). If resistance is encountered, cut fresh beveled tips on both the tubing and wire inset with sharp dissecting scissors.
- 3.4 Following the entry, withdraw the stylet and, using the dissecting microscope, confirm the presence of saliva at the puncture site. Avoid forceful or sudden movement (either withdrawal or insertion) of the stylet that may cause bleeding or compromise ductal integrity.
- 3.5 Retract the stylet within the tubing (Figure 3B).
- 3.6 To ensure that injection tubing will fit into Wharton's duct opening, insert tubing containing the stylet as a rigid guide into the previously made puncture (Figure 2C).

Note: If not performed quickly, local swelling may prevent re-insertion.
- 3.7 To prevent back pressure from prolonged ductal obstruction, withdraw the tubing. Inspect to verify that an opening, visible under microscopy, can be seen in the submandibular papilla. If visible bleeding occurs, remove the stylet and reattempt from step 3.2 on the opposing submandibular papillae.
- 3.8 Without moving the mouse, administer intraperitoneal injection of 1 mg/kg atropine solution, to reduce salivation during the procedure. Wait 5–10 min.
- 3.9 Grasp the end of the syringe tubing, and insert into the orifice using the dissecting microscope (Figure 3C). If resistance is encountered, cut a fresh beveled end to the tubing and reattempt.

- 3.10 Once the tubing is in place within the submandibular papilla, slowly advance 3–5 mm into the duct. Release the tubing from the forceps.
- 3.11 To improve the seal between the tubing and the submandibular papilla, dry the interface by gently blotting with gauze for 1 min.
- 3.12 Inspect to confirm that the position of the tubing has not shifted during drying.

4. Injection

- 4.1 Inject material at a rate of 10 $\mu\text{L}/\text{min}$. Inspect to confirm that the mouse remains sedated and is not showing signs of distress (Figure 2D).

Note: Injections of 15 – 50 μL are well tolerated. Injection of larger volumes can result in barotrauma.

- 4.2 Following the injection, maintain syringe pressure for 5 min to improve the retention of material within Wharton’s duct and SMG (Figure 4). Inspect the submandibular papilla periodically to ensure that tubing does not exit the ductal orifice.

- 4.3 Using fine forceps, grasp and gently withdraw the tubing from the submandibular papillae.

Note: It is normal to observe some fluid egress from the papillae.

- 4.4 Remove the retractor and cotton from the oral cavity before moving the mouse from the stage.

Note: The animal should not be left unattended until it has regained sufficient consciousness to maintain sternal recumbency. Furthermore, ensure that the mouse is not housed with other mice until fully recovered.

5. Verification and Analysis

Note: An *in vivo* Imaging System (IVIS) can be used to assess retention of fluorescently labeled nanoparticles following injection (as shown 1 h and 24 h after injection in Figure 5).

- 5.1 To better visualize fluorescent signal within the SMG through the skin, remove the ventral fur overlying the SMGs either by shaving or using a chemical depilatory.

Note: Following euthanasia, SMG tissue can also be harvested, fixed (overnight in 4% paraformaldehyde), and stained using immunohistochemistry to confirm persistence of fluorescently labeled NP one day following injection (Figure 6).

REPRESENTATIVE RESULTS

Retroductal injection can be used to administer NPs to the murine SMG (Figure 1). Here, we deliver 50 μg PSMA NPs labeled with Texas Red fluorophore.

Proper placement of the mouse allows facile access and visualization of the floor of the mouth (Figure 2A–B). The submandibular papillae are identified as two fleshy protrusions beneath the tongue. Following the cannulation (Figure 2C) and atropine injection, syringe tubing can be placed into the submandibular papillae (Figure 2D).

To facilitate the cannulation, a small puncture in the submandibular papilla is first made using the wire stylet inside of the catheter tubing (Figure 3A). Once this is done, the stylet should be retracted within the tubing to serve as a rigid guide while a larger opening is made (Figure 3B). The stylet has a diameter of 0.076 mm, while the catheter tubing has an outer diameter of 0.25 mm. Following the creation of this larger opening, the pre-loaded catheter tubing, attached to the injection syringe, can then be guided into the ductal orifice (Figure 3C).

Following the injection, it is recommended that the syringe be immobilized and injection pressure maintained. If the pressure is not applied, delivery will be successful, albeit with less efficiency and reproducibility. This is demonstrated by injecting 50 μ L of 1% toluidine blue dye bilaterally and observing fainter staining in the gland without maintained pressure following the injection (Figure 4).

To verify NP delivery, the IVIS can be used to detect fluorescent signal within the mouse, which is lateralized to the injected region 1 h post administration (Figure 5). This approach enables the confirmation without euthanizing the mouse and can be continued longitudinally until signal is no longer detectable^{26,27}.

To confirm NP persistence in the SMG 24 h following injection, glands can be sectioned, and viewed by fluorescent imaging. Aqp5 and Krt5 IHC mark secretory and ductal cells of the SMG, respectively, and show NPs in both compartments (Figure 6).

DISCUSSION

Retroductal injection is critical for localized drug delivery to the salivary gland. This technique has applications in screening therapeutic agents for conditions including Sjogren's syndrome and RIH^{9,10,28}. Direct drug delivery into the SMG via retroductal injection provides a key advantage over systemic administration in its potential to reduce off-target effects, including immune activation¹¹. The ability to maximize local drug delivery, without accumulation in surrounding tissues can also enable therapeutic testing in a wider dose range than could be achieved systemically.

We present this protocol, with troubleshooting and quality check steps, as a detailed and updated method to deliver polymeric nanomaterials through Wharton's duct to the murine SMG²⁰. For example, proper use of a wire guide facilitates cannula placement. Furthermore, by using dry blotting instead of cyanoacrylate glues to hold the cannula in place during the injection, the risk of mucosal trauma is minimized. This method can be used to treat mice with a range of compounds, and can be performed over multiple days with the same mouse to evaluate a timecourse of repeat administration¹¹.

Normal gland secretion will provide a simple and straightforward clearance mechanism for excess payload, though this strategy should be optimized for different applications by careful selection of injected substance and titration of atropine dosage. In this case, NPs persist in the SMG for at least 24 h. By using NPs capable of drug loading, or similar nanomaterials, future applications of this work include overcoming the solubility limit that would otherwise prevent testing hydrophobic agents with retroductal injection^{20,21}.

Acknowledgments

Research reported in this publication was supported by the National Institute of Dental and Craniofacial Research (NIDCR) and the National Cancer Institute (NCI) of the National Institutes of Health under Award Number R56 DE025098, UG3 DE027695, and F30 CA206296. The content is solely the responsibility of the authors and does not necessarily represent the official views of the National Institutes of Health. This work was also supported by the NSF DMR 1206219 and the IADR Innovation in Oral Care Award (2016).

We would like to thank Jayne Gavriety for her assistance in performing IVIS experiments. We would like to thank Karen Bentley for her input and assistance in performing EM. We would like to thank Pei-Lun Weng for his assistance with IHC. We would like to thank Matthew Ingalls for his assistance in figure preparation. We would like to thank Dr. Elaine Smolock and Emily Wu for critical reading of this manuscript.

References

1. Miranda-Rius J, Brunet-Llobet L, Lahor-Soler E, Farre M. Salivary Secretory Disorders, Inducing Drugs, and Clinical Management. *International Journal Of Medical Sciences*. 2015; 12(10):811–824. DOI: 10.7150/ijms.12912 [PubMed: 26516310]
2. Acauan MD, Figueiredo MAZ, Cherubini K, Gomes APN, Salum FG. Radiotherapy-induced salivary dysfunction: Structural changes, pathogenetic mechanisms and therapies. *Archives of Oral Biology*. 2015; 60(12):1802–1810. doi:<http://dx.doi.org/10.1016/j.archoralbio.2015.09.014>. [PubMed: 26454716]
3. Dirix P, Nuyts S, Vander Poorten V, Delaere P, Van den Bogaert W. The influence of xerostomia after radiotherapy on quality of life. *Supportive Care in Cancer*. 2008; 16(2):171–179. DOI: 10.1007/s00520-007-0300-5 [PubMed: 17618467]
4. Vissink A, et al. Clinical management of salivary gland hypofunction and xerostomia in head-and-neck cancer patients: successes and barriers. *International Journal of Radiation Oncology Biology Physics*. 2010; 78(4):983–991. DOI: 10.1016/j.ijrobp.2010.06.052
5. Delporte C, et al. Increased fluid secretion after adenoviral-mediated transfer of the aquaporin-1 cDNA to irradiated rat salivary glands. *Proceedings of the National Academy of Sciences*. 1997; 94(7):3268–3273.
6. Samuni Y, Baum BJ. Gene delivery in salivary glands: from the bench to the clinic. *Biochimica et Biophysica Acta*. 2011; 1812(11):1515–1521. DOI: 10.1016/j.bbadis.2011.06.014 [PubMed: 21763423]
7. Beahm DD, et al. Surgical approaches to the submandibular gland: A review of literature. *International Journal of Surgery*. 2009; 7(6):503–509. doi:<http://dx.doi.org/10.1016/j.ijsu.2009.09.006>. [PubMed: 19782158]
8. Zheng C, Shinomiya T, Goldsmith CM, Di Pasquale G, Baum BJ. Convenient and reproducible in vivo gene transfer to mouse parotid glands. *Oral diseases*. 2011; 17(1):77–82. DOI: 10.1111/j.1601-0825.2010.01707.x [PubMed: 20646229]
9. Zheng C, et al. Prevention of Radiation-Induced Salivary Hypofunction Following hKGF Gene Delivery to Murine Submandibular Glands. *Clinical Cancer Research*. 2011; 17(9):2842–2851. [PubMed: 21367751]
10. Okazaki Y, et al. Acceleration of rat salivary gland tissue repair by basic fibroblast growth factor. *Archives of Oral Biology*. 2000; 45(10):911–919. doi:[http://dx.doi.org/10.1016/S0003-9969\(00\)00035-2](http://dx.doi.org/10.1016/S0003-9969(00)00035-2). [PubMed: 10973565]

11. Arany S, Benoit DS, Dewhurst S, Ovitt CE. Nanoparticle-mediated gene silencing confers radioprotection to salivary glands in vivo. *Molecular Therapy*. 2013; 21(6):1182–1194. DOI: 10.1038/mt.2013.42 [PubMed: 23511246]
12. Cotrim AP, Sowers A, Mitchell JB, Baum BJ. Prevention of irradiation-induced salivary hypofunction by microvessel protection in mouse salivary glands. *Molecular Therapy*. 2007; 15(12):2101–2106. DOI: 10.1038/sj.mt.6300296 [PubMed: 17726456]
13. Redman RS, Ball WD, Mezey E, Key S. Dispersed donor salivary gland cells are widely distributed in the recipient gland when infused up the ductal tree. *Biotechnic & Histochemistry*. 2009; 84(6):253–260. DOI: 10.3109/10520290903081377 [PubMed: 19572222]
14. Grundmann O, Fillinger JL, Victory KR, Burd R, Limesand KH. Restoration of radiation therapy-induced salivary gland dysfunction in mice by post therapy IGF-1 administration. *BMC Cancer*. 2010; 10:417–417. DOI: 10.1186/1471-2407-10-417 [PubMed: 20698985]
15. Limesand KH, et al. Insulin-Like Growth Factor-1 Preserves Salivary Gland Function After Fractionated Radiation. *International Journal of Radiation Oncology Biology Physics*. 2010; 78(2): 579–586. doi:<http://dx.doi.org/10.1016/j.ijrobp.2010.03.035>.
16. Marmary Y, et al. Radiation-induced loss of salivary gland function is driven by cellular senescence and prevented by IL-6 modulation. *Cancer Research*. 2016
17. Baum BJ, et al. Early responses to adenoviral-mediated transfer of the aquaporin-1 cDNA for radiation-induced salivary hypofunction. *Proceedings of the National Academy of Sciences of the United States of America*. 2012; 109(47):19403–19407. DOI: 10.1073/pnas.1210662109 [PubMed: 23129637]
18. Arany S, et al. Pro-apoptotic gene knockdown mediated by nanocomplexed siRNA reduces radiation damage in primary salivary gland cultures. *Journal of Cellular Biochemistry*. 2012; 113(6):1955–1965. DOI: 10.1002/jcb.24064 [PubMed: 22253051]
19. Benoit DSW, Henry SM, Shubin AD, Hoffman AS, Stayton PS. pH-responsive polymeric siRNA carriers sensitize multidrug resistant ovarian cancer cells to doxorubicin via knockdown of polo-like kinase 1. *Molecular pharmaceutics*. 2010; 7(2):442–455. DOI: 10.1021/mp9002255 [PubMed: 20073508]
20. Malcolm DW, Varghese JJ, Sorrells JE, Ovitt CE, Benoit DSW. The Effects of Biological Fluids on Colloidal Stability and siRNA Delivery of a pH-Responsive Micellar Nanoparticle Delivery System. *ACS Nano*. 2017
21. Baranello MP, Bauer L, Benoit DS. Poly(styrene-alt-maleic anhydride)-based diblock copolymer micelles exhibit versatile hydrophobic drug loading, drug-dependent release, and internalization by multidrug resistant ovarian cancer cells. *Biomacromolecules*. 2014; 15(7):2629–2641. DOI: 10.1021/bm500468d [PubMed: 24955779]
22. Wang Y, et al. Fracture-Targeted Delivery of β -Catenin Agonists via Peptide-Functionalized Nanoparticles Augments Fracture Healing. *ACS Nano*. 2017; 11(9):9445–9458. DOI: 10.1021/acsnano.7b05103 [PubMed: 28881139]
23. Baranello MP, Bauer L, Jordan CT, Benoit DSW. Micelle Delivery of Parthenolide to Acute Myeloid Leukemia Cells. *Cellular and Molecular Bioengineering*. 2015; 8(3):455–470. DOI: 10.1007/s12195-015-0391-x [PubMed: 29552235]
24. Kuriki Y, et al. Cannulation of the Mouse Submandibular Salivary Gland via the Wharton's Duct. *Journal of Visualized Experiments*. 2011; (51):e3074.
25. Nair RP, Zheng C, Sunavala-Dossabhoj G. Retroductal Submandibular Gland Instillation and Localized Fractionated Irradiation in a Rat Model of Salivary Hypofunction. *Journal of Visualized Experiments*. 2016; (110)
26. Wang Y, Malcolm DW, Benoit DSW. Controlled and sustained delivery of siRNA/NPs from hydrogels expedites bone fracture healing. *Biomaterials*. 2017; 139(Supplement C):127–138. doi:<https://doi.org/10.1016/j.biomaterials.2017.06.001>. [PubMed: 28601703]
27. Hoffman MD, Van Hove AH, Benoit DSW. Degradable hydrogels for spatiotemporal control of mesenchymal stem cells localized at decellularized bone allografts. *Acta Biomaterialia*. 2014; 10(8):3431–3441. doi:<https://doi.org/10.1016/j.actbio.2014.04.012>. [PubMed: 24751534]

28. Nguyen CQ, Yin H, Lee BH, Chiorini JA, Peck AB. IL17: potential therapeutic target in Sjogren's syndrome using adenovirus-mediated gene transfer. *Laboratory Investigation*. 2011; 91(1):54–62. DOI: 10.1038/labinvest.2010.164 [PubMed: 20856230]

Author Manuscript

Author Manuscript

Author Manuscript

Author Manuscript

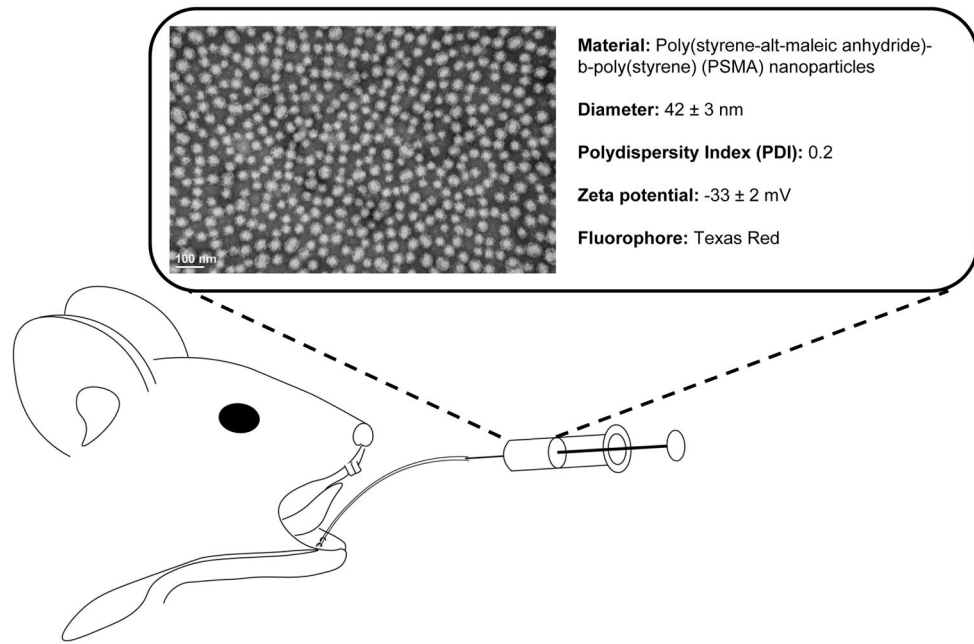


Figure 1. Retrograde injection schematic

Following ductal cannulation and syringe placement, 50 μ L of 1 mg/mL polymeric NP solution is injected into the SMG. Representative transmission electron micrograph (TEM) shows monodisperse (polydispersity index = 0.2) NP population.

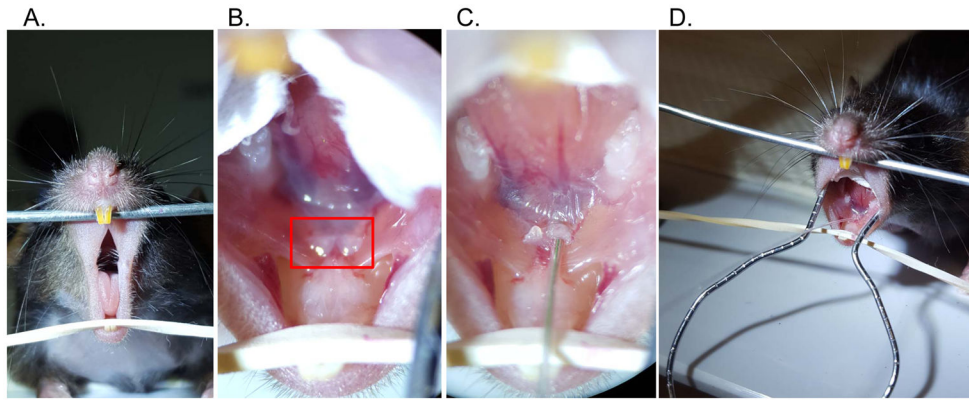


Figure 2. Retrograde injection steps

A. Access the oral cavity by separating the maxillary and mandibular incisors. B. Visualize the papillae (boxed) below the tongue at the floor of the mouth, which mark the location of Wharton's duct. C. Using a catheter with wire inset, gently cannulate the base of the submandibular papilla. D. Following cannulation, the catheter tubing can be exchanged with syringe tubing

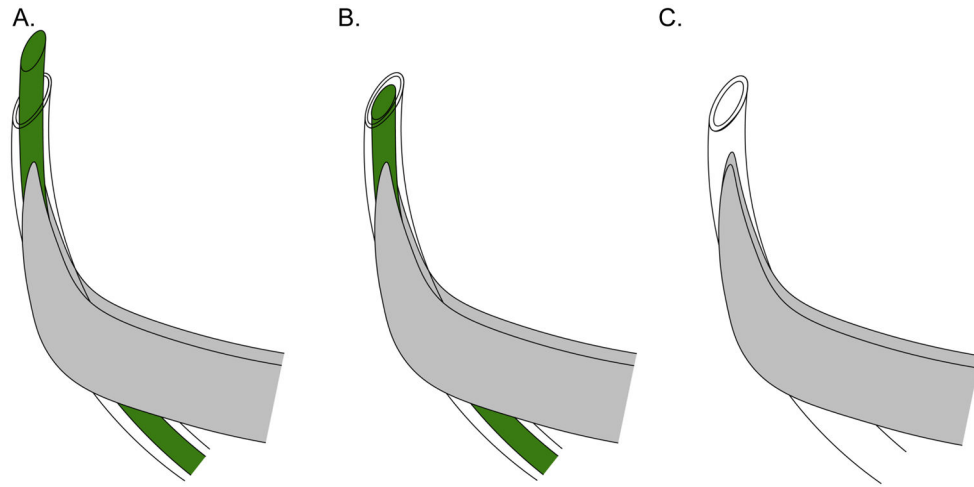


Figure 3. Effective positioning of catheter and stylet for Wharton's duct cannulation

A. Align the tubing with the curvature of the forceps, and cut a beveled end on the tubing and wire to initially puncture the sublingual papilla. B. Retract the stylet within the tubing to make a rigid guide to insert the tubing within the sublingual papilla. C. Insert catheter tubing (stylet removed), joined to injection syringe, within the previously made orifice.



Figure 4. Maintaining syringe pressure following injection improves material retention
Following retroductal injections of 50 μL of 1% toluidine blue, syringe pressure was either maintained for 5 min (Right SMG – first injection) or the syringe was withdrawn immediately after the injection (Left SMG – second injection).

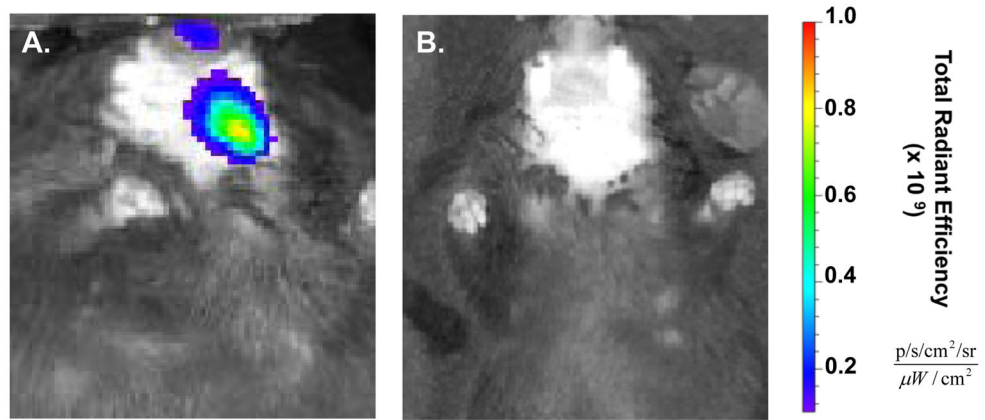


Figure 5. Confirmation of retroductal NP delivery post injection

A. *In vivo* Imaging System (IVIS) shows the lateralization of red fluorescent signal to the treated (left) side of the mouse 1 h post injection. B. NP IVIS signal at 24 h has decreased significantly.

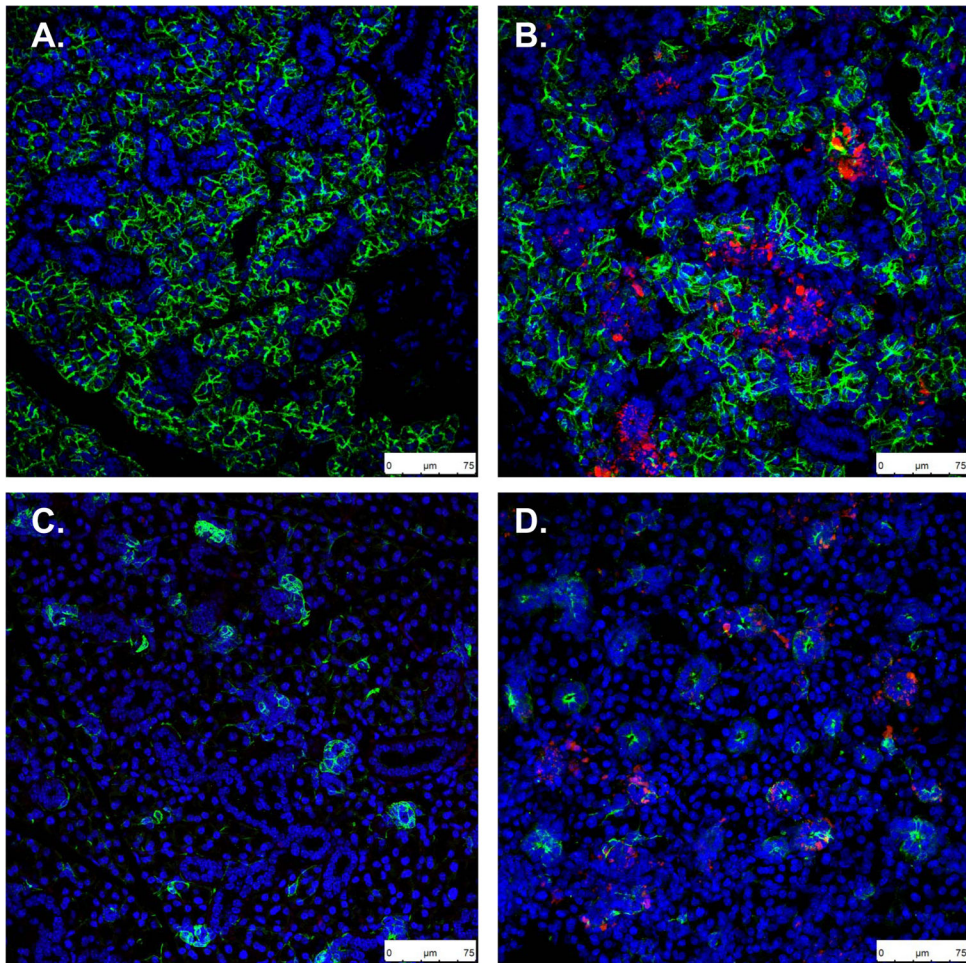


Figure 6. Confirmation of retroductal NP persistence 24 h post injection

A, C. Uninjected control SMG stained for Aqp5 and Krt5, marking secretory acinar and ductal cells, respectively. B, D. In retroductal NP injected SMG, Aqp5 and Krt5 stains show normal gland morphology and NPs taken up in both acini and ducts (scale bars: 75 μm).